Light Metals 2011 *Edited by: Stephen J. Lindsay*
TMS (The Minerals, Metals & Materials Society), 2011

MOULD WALL HEAT FLOW MECHANISM IN A DC CASTING MOULD

A. Prasad[1], I.F.Bainbridge[1].
[1]CAST CRC, University of Queensland, Brisbane, QLD 4072, Australia

Keywords: DC casting, Mould-wall, Heat Flow, Radiation

Abstract

Experiments have been performed to study the effect of the mode of heat transfer on the heat flow in the wall of a DC casting mould. Billet casting uses graphite as inner lining material within the mould-wall. Graphite being a black-body, provides a possible pathway for radiation to play a role in the mould-wall heat transfer. As such, experiments were performed with a graphite probe on the experimental apparatus presented at TMS 2010. An overview of these results will be presented together with the implications of the results for the DC casting process.

Introduction

The practice of DC casting of aluminium and aluminium alloys requires the removal of heat from the surface of the solidifying metal at two points within the system: the sub-mould cooling impingement area (often referred to as the primary cooling zone) and the mould wall area. Heat flow in the sub-mould cooling area has been reasonably well studied and confirmed values are available for the heat transfer coefficient for a range of casting conditions [1-4]. Several estimates of the mould wall heat transfer have been made, together with some attempts to measure the heat flow during an actual cast. The amount of heat flow is characterized by the heat transfer coefficient and Table I summarizes the current data available.

Table I. Published values for mould wall heat flow

Parameter	Value	Units	Ref.
Heat transfer coefficient – molten metal to mould	2000 3000 2400 1000 1000–2000 650 – 1600	$Wm^{-2}K^{-1}$	[1] [2] [3] [4] [5] [6]
Heat transfer coefficient – air gap formed in mould	200 250 – 350	$Wm^{-2}K^{-1}$	[1] [2]
Heat flux – molten metal to mould wall – *Hot top casting* *Air pressurized casting* *Rolling block casting – Sumitomo*	 1270 420 ~800	kWm^{-2}	 [4] [4] [7]
Rate of heat removal through the mould (for 152mm dia. 6063 billet cast at 101, 152 & 228 mm/min.)	7,600 (9.1%) 11,000 (9.0%) 18,000 (10.4%)	W (% of total)	[8]

Knowledge of the actual heat flow from metal to the mould wall and the factors that influence this are thought to be important for both the design and operation of a DC casting mould [9, 10]. Cast product quality has been directly linked to the amount of heat removed through the mould wall [4, 11]. Moreover, accurate simulation of the process by mathematical modeling is dependent upon reliable data for this factor.

CAST CRC initiated research in this direction to endeavor to quantify some of the important factors that can possibly influence the mould-wall heat flow in a DC casting. However, the measurement of the mould wall heat flow under controlled conditions during an actual DC cast is extremely difficult and costly. Determination of the effect of individual factors that may have an influence on the mould wall heat flow is not possible under such conditions. Hence, at CAST, the focus has been to develop a laboratory simulation of an operating mould and to use this to accurately measure the heat transfer coefficient between the molten metal and the simulated mould wall under a range of controlled conditions known to occur within a DC casting mould.

The essentials of the experimental apparatus were described in the previous work [12]. It is also briefly described here under "Equipment design and operation" section. Initial experiments were done with an AA601 probe on two sample types - 99.85% Al sample (molten metal at ~700 °C) and stainless steel samples (solid sample at 700 °C). Note that the AA601 alloy probe is the same material from which industrial moulds are made. The first set of experiments was performed by passing dry air @ 1.0 lpm between the probe and the sample. Further experiments were performed with different gases at the same flow rate namely, nitrogen, argon, and carbon-dioxide with stainless steel samples. The reason for using a stainless steel sample was to mitigate the difficulty of obtaining a flat sample surface with molten metal samples and hence a more accurate sample/mould gap [12]. The experimental results obtained for experiments with different gases on the stainless steel samples are repeated here in Figure 1 for convenience.

The results clearly showed a linear correlation between the heat transfer coefficient and the gas thermal conductivity. Thus the conduction mechanism was suggested to be dominant. However, since a billet mould for a DC casting has a graphite lining, graphite being a black-body (emissivity ≅ 1 [13]), potentially provides a pathway for radiation to play a role in the heat transfer. From the previous experiments with an AA601 alloy probe, the effect of radiation in the metal-probe gap heat transfer was not clear. To study the effect of radiation, further experiments were planned with a graphite probe with the same design features as the AA601 probe.

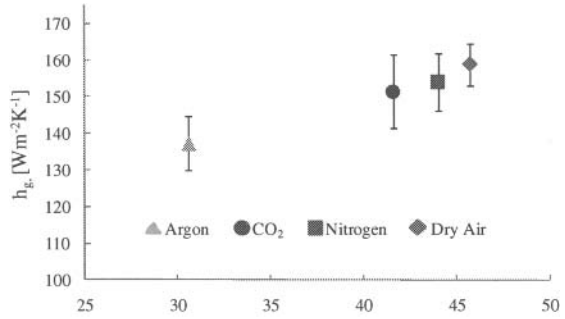

Figure 1. Heat transfer coefficient versus mould gas thermal conductivity for a constant 0.5 mm gap [12]. Sample = stainless steel, probe material = AA601

Equipment design and operation

The basic concepts of the experiments are the same as reported earlier [12]. The experiment attempts to simulate the heat flow during an actual DC casting operation. During DC casting, as molten metal is poured into the mould, a liquid meniscus is formed which has a variable gap between it and the mould wall. Concurrently, the molten metal at higher temperature loses heat through this gap to the mould. This heat flow translates to a temperature gradient within the mould. This situation can be simulated in a laboratory experiment by using a thermal probe as analogous to a mould and subsequently measuring the temperature gradient within the probe. This was explained in the previous publication [12].

The experimental apparatus consists of a water cooled probe (AA601 or graphite) with thermocouples embedded facing a sample (pool of molten 99.85%Al or solid steel sample – both at 700 °C). The gap between the probe and the sample is continuously changed and the resulting heat flow through the probe is captured by the thermocouples which record the proportional temperature gradient within the probe.

Knowing the temperature difference (ΔT_2) across the probe (from the sample facing front face to the water cooled rear section, i.e. distance L_2) and the temperature difference between the front face of the probe and the sample (ΔT_1), the heat transfer coefficient (h_g) can be calculated using Fourier's law, by first determining the quantity of heat, Q, flowing through the probe.

$$Q = \frac{kA}{L_2}(\Delta T_2) \tag{1}$$

This is then converted to a heat flux ($q = \frac{Q}{A}$) and then

$$q = h_g\left(T_{metal} - T_{mould}\right) = h_g \Delta T_1 \tag{2}$$

is used to determine the heat transfer coefficient, h_g. In these equations, k is the thermal conductivity of the mould material and A is the mould surface area through which heat is transferred.

In the reported experimental work, these equations were used to determine h_g across a fixed (but adjustable) distance between a the sample surface and the probe. This feature makes this steady-state experiment unique in that the other experiments reported in the literature only estimate transient values of h_g [5,14], whereas our values were for steady-state conditions. The effect of the metal-probe gap on h_g for the present work is therefore unequivocal.

The experimental procedure details were the same as in the previous experiments [12]. Thus the sample temperature was kept constant at ~700 °C, the gas flow rate was fixed at ~1.0 lpm etc. The choice of sample type used for the current experiments is described later. Also, the data gathering and recording of different parameters viz., ΔT_1, ΔT_2, L_1 etc. mentioned in equations 1 and 2, were performed in the same manner. The probe features were also kept the same as before (Figure 2). A Tokai grade G384 graphite was used for the probe with a thermal conductivity of 128 Wm^{-1}K^{-1}. However, because of the brittleness of graphite, the probe broke at several thin sectioned regions during installation. It was decided to redesign a slightly bigger probe with thicker sections for structural rigidity. The essential features of embedded thermocouples, water cavity etc., from the original probe was kept the same.

Figure 2 shows the schematic of the previous probe. For the present set of experiments, the flange section of the probe attaching to the top plate was made thicker since this section was the most vulnerable. The region in the probe where the thermocouples were embedded was also lengthened slightly to enable embedding 3 thermocouples instead of 2 thermocouples previously. This allowed a check on the thermocouple data since the temperature gradient between thermocouples 1-2 should be the same as that between thermocouples 2-3. The new probe was therefore slightly longer in length (from the top plate to the face) compared to the earlier version. The rest of the design features were kept the same.

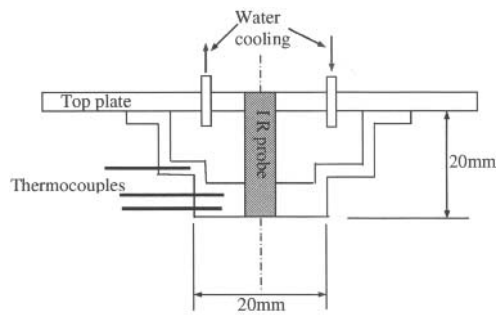

Figure 2. Drawing of the probe showing the positions of the three thermocouples and water cooling.

There were some changes in the experimental plans which were deemed important. Firstly, the previous results were quoted for stainless steel samples. However, it was considered important to perform experiments with an aluminum based sample, simply because of its direct relevance to the actual DC casting situation. Secondly, since the probe dimensions were changed, albeit slightly, it was considered important to perform experiments with a similarly modified AA601 probe so that a direct comparison between probe material types could be made. Thus experiments

were performed with molten 99.85-wt%Al in dry air and argon with both AA601 and graphite probes to the modified design.

Results

The results for each particular set of experimental conditions (probe material type and mould gas) were plotted and the trend line equations then used to calculate h_g at a particular mould gap. It was mentioned in the previous work that the heat transfer coefficient varied non-linearly with the gap, but had a linear co-relation with the inverse of the gap [12]. As the inverse relationship (h_g vs 1/gap) is a straight line this was used for the data analysis. The equation thus obtained was used to calculate the heat transfer coefficient, h_g, at 0.5mm probe-metal gap. The following figures show the plots between h_g vs 1/gap from which equations and R^2 values were generated using linear regression analysis. These equations were then used to estimate the h_g values at 0.5mm gap (reported in Table II).

Figure 3 shows the results from experiments with molten 99.85-wt%Al sample at 700 °C facing a AA601 alloy probe in dry air and argon. The figure plots the heat transfer coefficient as a function of the inverse of the gap. The heat transfer coefficient between the molten metal and the mould wall in a DC casting mould was found to be dependent upon the size of the gap between the molten metal and the mould wall [12]. The same result is seen here, which is a validation for the modified probe working correctly (similar R^2 values approaching 1 were obtained with both the older and the modified version of the probe).

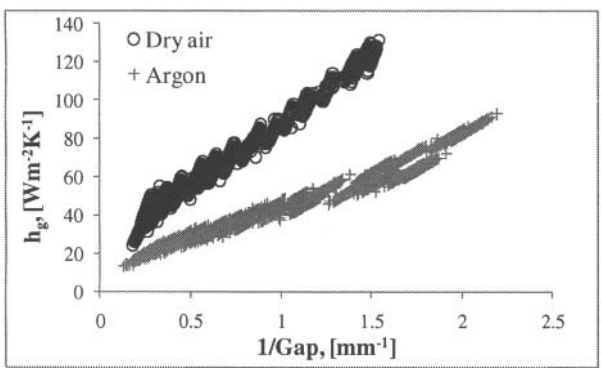

Figure 3. Plot showing the heat transfer coefficient as a function of inverse of mould gap – AA601 probe, 99.85%Al.

Likewise, Figure 4 shows the same results for the 99.85-wt% Al in dry air and argon respectively with the graphite probe. A similar trend is seen as with the AA601 probe. In each of the sets of plots in Figures 3-4, there are approximately 5000 data points. A single run produces approximately 2250 data points of heat transfer coefficient vs gap (or the inverse of the gap). And for each combination of probe material type and gas type, at least 6 runs were performed. Therefore, the plots show only a fraction of the data points actually obtained. A tight band of data points for a given set of experimental conditions shows the consistency of the experiments. Note that all the successful experiments showed a similar plot with closely bound data points within a given set.

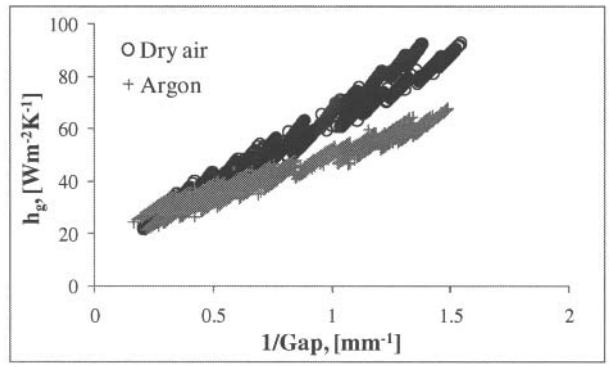

Figure 4. Plot showing the heat transfer coefficient as a function of inverse of mould gap – Graphite probe, 99.85%Al.

For both the figures (3 and 4) there is a clear difference in slopes for the two gases tested. This replicates the effect of gas type as seen in Figure 1 for the steel samples with the older probe. Furthermore, considering the effect of probe material types, the y-axis scales are different for the two figures. The highest value in the scale shows that the graphite probe gives slightly lesser values of h_g as compared to the AA601 probe. This difference is seen more clearly in Table II.

Table II compares the results from the AA601 and graphite probe for the two gases. The average values of h_g at a mould gap of 0.5mm are quoted with all the data points taken into the calculations. The h_g values were obtained by using the linear least square regression lines for each set of data points i.e. [AA601 probe, 99.85-wt%Al, dry air] as stated before. Also included in the table is the percentage difference in conductivity between the two gas types and the probe material types. The gas conductivity values were evaluated at 600K, which is approximately the average of the sample temperature (700 °C ≅ 975K) and the probe surface temperature (~40 °C maximum ≅ 310K).

Table II. Heat transfer coefficient, h_g for different combinations of probe material and gas types.

Gas type / Probe material	h_g, [Wm^{-2}K^{-1}] (at 0.5mm)		% diff. h_g (probe mtl.)	% diff Gas cond., k_g	% diff Probe cond. k
	AA 601	Graphite			
Dry air	148.3±18.9	125±10.2	15.7%	33.0%	19.5%
Ar	88.3±9.8	86.9±8.0	1.5%	33.0%	19.5%
% diff. h_g (gas)	40.5%	30.5%	-	-	-

The effect of radiation may be manifested in two ways – one due to the radiative properties (absorption, reflection etc.) of the mould material (probe material in our case) and the other due to the emissivity of the molten metal (sample in our case). Therefore, the results from the four sets of experiments were also compared with the steel sample results in Figure 1. Note that Figure 1 was based on an earlier version of the probe, and also, had data for four different gas types. Nevertheless, a comparison is valid for two reasons. Firstly, the modified probe gives similar trends as the older probe, therefore the working of the two probes were not

vastly different. Moreover, only a small change was made in the new probe. Secondly, given that the old and the new probe yield similar results, the comparison provides an opportunity to compare two different sample types, steel and aluminum, whose oxides are very different. Thus the comparison provides more information to compare the radiation component of heat transfer via differences in the emissivity of the two oxides.

Figure 5 shows this comparison. A theoretical set of data points are also plotted. The theoretical data points were based on the Ho-Pehlke [15] prediction of h_g for steady state conditions. Their model is simply given by: $h_g = k_g/gap$, where k_g is the gas conductivity. For our case, the gap was fixed at 0.5mm.

Discussion and Conclusions

From Figures 3-4 and Table II it is clear that there was a difference in the amount of heat flow across the gap when the gas type and/or the probe material was changed. In Figure 3, as the gas type was changed, the slope of the data points changed, showing a smaller hg value for Ar. The same trend was seen in Figure 4. There seems to be a larger change in the slope for the AA601 probe as compared to the graphite probe. However, from Table II it is clear that for either of the probe types, the change in h_g values due to a change in gas type was similar (30 – 40%). This was close to the difference in the gas conductivity between dry air and Ar (33%). Note that the percent difference was based on the average h_g values.

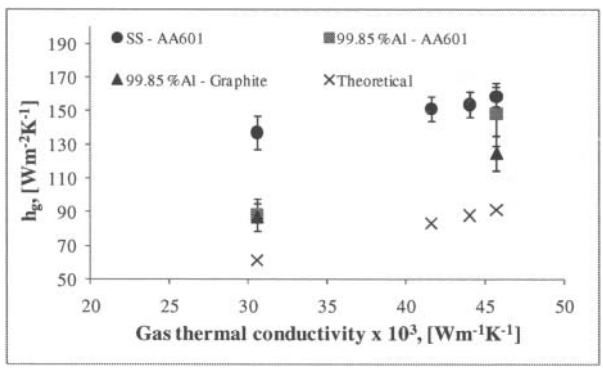

Figure 5. Comparison of h_g values versus mould gas thermal conductivity for a constant 0.5 mm gap with different probe/sample combinations.

On the other hand, the effect of difference in probe material was not as straightforward. For example, for dry air, the difference between hg values from AA601 and graphite probe was ~16%, but it dropped to 1.6% for the Ar gas. Note that the difference in the probe material conductivity was ~20%. In other words, the difference in probe material conductivity had been overridden by the gas type. Thus the gas conductivity seems to have been the more dominant parameter.

Effect of radiation:

Before discussing the effect of radiation, it should be mentioned that there had been a limited number of experiments on the steel sample with different gas flow rates (0-3 lpm). The flow rates were so chosen as to simulate the range of flow rates normally encountered within a DC casting mould. These runs showed that the h_g (at 0.5mm) values were not affected within this range of flow rates. This suggests that the convection effects (forced or natural) were negligible. Hence any difference in the h_g values between various combinations of sample type, gas type or probe type must have been a result of major contributions from conductivity and radiation mechanisms only. The effect of gas conductivity on h_g values has already been demonstrated.

For a given gas type, when the results between different sample types are compared, the following comparisons can be made. Within the Al-based samples, the results can be compared between the two different types of probe. For the two probes, the hg values were similar, particularly for Ar. For this case, as discussed earlier, it transpires that the gas conductivity was the dominant mechanism. This suggests that the material of the probe did not play a major role in the heat transfer. In other words, the absorptivity and reflectivity properties of the mould material may be of minor consequence in a DC casting operation.

The second comparison is that between the steel and Al sample for the AA 601 probe for the two different gases. It can be seen that for a given gas type, the steel samples had higher values than the Al samples. Since the conductivity is the same for the gas type, by elimination, the difference must be attributed to the radiation. Literature [16] suggests that the emissivity of an oxide layer between stainless steel and molten aluminium will be different. However, this is a function of the temperature and the degree of oxidation. A higher degree of oxidation in steel would result in a higher emissivity of the oxide layer. In our experiments, the molten metal was skimmed prior to the start of each run, but the steel sample surface was left untouched between runs. Note that the literature search on emissivity was performed much later and therefore at the time of performing steel runs, the authors were unaware of the effect of oxidation on the emissivity of oxide of the steel. The literature [16] also suggests that beyond ~800K, highly oxidized steel would have higher emissivity than aluminium oxide. Our experiments were performed at ~975K, which is well over the 800K limit suggested in the literature.

It is interesting to note that for dry air, the h_g values between Al and steel were not vastly different. However, for Ar, this difference increased markedly. While difference in emissivities can be attributed to explaining the difference in h_g values between Al and steel for dry air, differences in emissivities fail to explain the large difference in hg values for Ar.

The overall mechanism seems to be gas conduction dominated. On the other hand, radiation can affect the gas molecules by transferring energy to the molecules, thereby heating them. This in turn would affect the conduction since conduction through a gaseous medium relies on molecular movement. Since both the probe face and the sample had a finite area (ϕ = 20mm each), the view factor could be an issue as well. The view factor will change with a change in gap (increases as the metal-probe gap decreases). Thus at smaller gaps the effect of radiation on Argon's conductivity could be higher than that for dry air. For our experiments with dry air and Ar, such effects of radiation on conduction have not been determined.

This would require an in-depth study, perhaps a modeling effort to quantify such an effect of radiation. Also, a more rigorous quantitative analysis can be performed by doing radiation-focused

experiments in a high vacuum. In such a situation, with absence of gas molecules, the conduction and convection components will be negligible with radiation the major mechanism. However, a high vacuum is not easy to obtain and this would also require major changes in the experimental set-up. As such, the vacuum based experiments have not been performed at this time. Thus at this stage it is only possible to conclude that radiation has a definite effect on the heat transfer via differences in emissivities of the sample type.

Implications for DC casting:

The aluminium sample results with different probe types showed a small difference in h_g, which was not large enough to cause a major difference in the heat extraction through the mould wall. Recall that the majority of the heat extraction in DC casting is through the sub-mould water jets. However, the effect of the gas conductivity has been shown to be quite pronounced. Hence it is suggested that in the situation where vapors from the oil, steam from sub-mould cooling etc. are present in the metal-mould gap, the heat extraction through the mould gap will be affected. Finally, the type of metal cast may or may not have an effect depending upon the emissivity of the oxide skin formed. The effect of oxide skin on radiation emissivity also requires in-depth study in terms of the variables, namely: amount of oxidation, the chemical composition, crystal structure of the oxide etc. In another aspect of the present work, the h_g for different aluminium alloys in dry air had been determined. In cases where high levels of Mg and or Zn are present, e.g., 5xxx or 7xxx series alloys, a thicker, more adherent oxide film was formed, along with some difference in the h_g values. The results of this work are yet to be reported.

In summary, a new technique has been developed that enables the measurement of heat transfer across a simulated metal-mould gap for a DC casting. In the present work, this technique has been used to study the effect of radiation on the heat transfer across the gap. This was done by performing experiments on Al-samples under two different gases with two different probes – AA 601 and graphite. It was found that radiation had a small effect on the heat transfer coefficient via emissivity of the sample. The absorption/reflection of the probe body did not have any noticeable effect. Overall, the effect of radiation resulted in a small difference. However, it is suggested that this difference is not sufficient to cause a significant change in mould wall heat transfer in an actual DC casting. To accurately quantify the effect of radiation, further work (experimental/theoretical or both) is required.

Acknowledgements

CAST CRC was established under, and is funded in part by the Australian Federal Government's Cooperative Research Centre scheme.

References

1. A. Sabau et al, "Heat Transfer Boundary Conditions for the Numerical Simulation of the DC Casting Process", ed. A.T.Taberaux (Charlotte, NC: Light Metals, TMS, 2004), pp.667-672.
2. D. Mortensen, "Mathematical model of the heat and fluid flows in direct-chill casting of aluminum sheet ingots and billets", *Metallurgical Transactions B*, 30B (1999), 119-133.
3. J. M. Drezet et al, "Determination of thermophysical properties and boundary conditions direct-chill cast aluminium alloys using inverse methods", *Metallurgical Transactions A*, 31A, (2000) 1627-1634.
4. J. F. Grandfield, and P. T. McGlade, "DC casting of aluminium: Process behaviour and technology", *Materials Forum*, 20 (1996), 29-51.
5. K. Ho, and R. D. Pehke, "Metal mould interfacial heat transfer", *Metallurgical Transactions B*, 16B (1985), 585-594.
6. M. Trovant, and S. Argyropoulos, "A Technique for the Estimation of Instantaneous Heat Transfer at the Mould/Metal Interface During Casting", ed. R. Huglen (Orlando, Florida: Light Metals, TMS, 1997), 927-931.
7. N. Muto, N. Hayashi, T. Uno, Sumitomo Light Metals Technical Reports 37 (1996) 180-184.
8. D. C. Weckman, and P. Niessen, "Numerical simulation of the DC continuous casting process including nucleate boiling heat transfer", *Metallurgical Transactions B*, 13B (1982), 593-602.
9. P. W. Baker, J. F. Grandfield, "Mould Wall Heat Transfer in Air-Assisted DC Casting", *Solidification Processing*, (London UK: 3rd Conference, The Institute of Metals, 1987), 257-260.
10. M. Ekenes, W. S. Peterson, "Visual Observations Inside an Airslip Mould During Casting", ed. C. Bickert (Anaheim, California: Light Metals, TMS, 1990), 957 - 961.
11. S. Instone, W. Schneider, and M. Langen, 'Improved VDC Billet Casting Mould for Al-Sn Alloys", ed. P. N. Crepeau (San Diego, California: Light Metals, TMS, 2003), 725-731.
12. A. Prasad, J. Taylor, I. Bainbridge, The Measurement of Heat Flow within a DC Casting Mould, ed. J. A. Jensen, (Seattle, WA: Light Metals, TMS, 2010), 765-770.
13. Michael F. Modest, *Radiative Heat Transfer* (Academic Press, 2003), 746-752.
14. M. Trovant, and S. Argyropoulos, "Finding Boundary Conditions: A Coupling Strategy for the Modeling of Metal Casting Processes: Parts I and II", *Metallurgical Transactions B*, 31B (2000), 75-96.
15. K. Ho, and R. D. Pehlke, "Transient methods for determination of metal-mould interfacial heat transfer", *AFS Transactions*, 92 (1984), 587-598.
16. Frank P. Incropera, and DavidP.Dewitt, *Fundamentals of Heat and Mass Transfer* (John Wiley and Sons, 1990), 722-723.